Electronic Supporting Information

Hydrogenation of levulinic acid to γ-valerolactone over single-atom Pt confined in Sn-modified MIL-101(Fe)

Runze Zhang,[‡] Yinghao Wang,[‡] Wendi Zhang, Yaowei Lu, Qinghu Tang, Qiue Cao, Bang Gu,[*] and Wenhao Fang[*]

[‡] These authors contributed equally to this work.

[*] Corresponding authors. E-mail addresses: gubang@ynu.edu.cn; wenhao.fang@ynu.edu.cn.

1. Experimental details

Materials and reagents

All the chemicals were directly used as received without further purification or treatment. $H_2PtCl_6 \cdot 6H_2O$ (99.9%), $Fe(NO_3)_3 \cdot 9H_2O$ (98%), α-angelica lactone (α-AL, 98%) and 1,4-dioxane (>99%) were obtained from Alfa Aesar. Levulinic acid (LA, 99%), $SnCl_2 \cdot 2H_2O$ (98%) and γ-valerolactone (GVL, >98%) were purchased from Adamas Reagent. Terephthalic acid (99%), $NaBH_4$ (98%), acetic acid (99.5%) and *N,N*-dimethylformamide (DMF, 99.9%) were obtained from Innochem.

Catalyst preparation

The Sn-modified MIL-101(Fe) carriers with variable Sn/Fe molar ratios (*i.e.*, 0.1, 0.2 and 0.3) were prepared by hydrothermal method. In brief, with the $MIL(FeSn_{0.2})$ carrier as an example, $Fe(NO_3)_3 \cdot 9H_2O$ (5 mmol), $SnCl_2 \cdot 2H_2O$ (1 mmol) and terephthalic acid (6 mmol) were dissolved in 25 mL of DMF, and then 5 mL of acetic acid was added slowly under stirring (600 rpm). Subsequently, the slurry was stirred at 25 °C for 30 min, and then it was transformed into a 100 mL of Teflon-lined autoclave and maintained at 120 °C for 24 h. After cooling to 25 °C, the obtained brown-yellow solids were collected by centrifugation and washed three times with DMF. In order to completely remove DMF, the solids was dispersed in 40 mL of methanol and then refluxed at 65 °C for 12 h. Finally, the carrier separated by filtration was dried under vacuum at 80 °C for 2 h, and named as $MIL(FeSn_x)$, where x represents the Sn/Fe molar ratio. MIL(Fe) and MOF(Sn) as the referenced carriers were prepared by the same procedure.

$MIL(FeSn_x)$-encapsulated Pt catalyst (Pt loading: 0.5 wt.%) was prepared by adsorption method. In brief, 1 mL of $H_2PtCl_6 \cdot 6H_2O$ solution (Pt: 4.76 mg mL^{-1}) was added to 100 mL of distilled water in a brown flask. The solution was stirred for 15 min at 25 °C, and then 476 mg of $MIL(FeSn_x)$

carrier was dispersed in the solution and stirred for another 8 h (600 rpm). The obtained brown solids were separated by filtration and washed repeatedly by adequate water and ethanol to entirely remove Cl⁻ ions. Finally, the Pt@MIL(FeSn$_x$) catalyst was dried at 80 °C under vacuum for 8 h. Pt@MIL(Fe) and Pt@MOF(Sn) as the referenced catalysts were prepared by the same method.

Catalytic reaction

LA (5 mmol), catalyst (50 mg) and 1,4-dioxane (10 mL) were mixed and sealed into a batch-type Teflon-lined stainless-steel autoclave (50 mL). After purge and introduction of H$_2$ at a pressure of 1 MPa, the reactor was then placed in an oil bath pre-heated at 100 °C with a magnetic stirring at 800 rpm. When the reaction was over, the reactor was rapidly placed in an ice-bath. And then the used catalyst was separated by filtration and washed by hot distilled water and ethanol for three times followed by drying at 80 °C under vacuum for 8 h before the next use.

The reactant and products were analyzed on a Thermo Scientific TRACE 1310 gas chromatograph (GC) armed with a flame ionization detector (FID) and a TR-5 column (30 m, 0.32 mm, 0.25 μm). The quantification was carried out on an external standard method by calibrating the standard solution at different concentrations for LA, α-AL and GVL. Conversion of reactant and selectivity of each product were defined as the molar percentage of reactant converted and the molar percentage of each product formed in reactant converted, respectively. Both conversion and selectivity were calculated on a carbon basis. Notably, the carbon balance was monitored for each reaction, and the obtained data were of 99–100% (not reported in figures and tables), which revealed that the reported catalytic performances are reliable. Each reaction was repeated at least twice to guarantee a reproducible result, and the error of the data must be no more than 2%. Conversion of LA, selectivity of products, initial reaction rate (r), and intrinsic turnover frequency (TOF) were calculated by the following equations.

$$Conv. \, (\%) = \frac{n_{LA,initial} - n_{LA,final}}{n_{LA,initial}}$$

$$Select. \, (\%) = \frac{n_{product}}{n_{LA,initial} - n_{LA,final}}$$

$$r \left(mol \, mol_{Pt}^{-1} \, s^{-1}\right) = \frac{n_{LA,initial} - n_{LA,final}}{n_{Pt} \times time}$$

$$TOF \, (h^{-1}) = \frac{initial \, conversion \, rate \, \times \, M_{Pt}}{Pt \, dispersion}$$

Characterization methods

Powder X-ray diffraction (XRD) was carried out using a Rigaku TTR III Diffractometer provided with Cu Kα radiation (λ = 1.5418 Å) and a beam voltage of 40 kV. The patterns were recorded in the 2θ domain (10–90°) with a measured step of 0.02° and a time integration of 0.2 s. The specific surface area of MIL(FeSn$_x$) carrier was calculated by BET method from N$_2$ adsorption-desorption isotherm recorded at 77 K on a Micromeritics TriStar II 3020 Surface-Area Analyzer. The pore volume and pore size were calculated by HK method. The loadings of Pt, Sn and Fe were determined by Inductively Coupled Plasma Mass Spectrometry (ICP-MS) using an Agilent 7500a apparatus. The solid sample was thoroughly dissolved by a mixed acid of HCl and HNO$_3$, and the obtained solution was placed at room temperature overnight. X-ray photoelectron spectroscopy (XPS) analysis was performed under ultra-high vacuum on a Thermo Scientifc Escalab 250Xi system equipped with Al Kα radiation. The binding energy (BE) shift due to the surface charging was adjusted based on a reference to the C 1s line at 284.5 eV. Transmission electron microscopy (TEM) measurement was conducted on a Philips-FEI TECNAI F30 field-emission electron microscope operated at an acceleration voltage of 300 kV. HAADF-STEM was performed on an atomic resolution analytical microscope (JEM-ARM 300 F) operating at 300 kV. Energy dispersive

spectroscopy (EDS) was collected on JEM-ARM 300 F operating at 80 kV. Samples were previously suspended in ethanol and dispersed ultrasonically. Drops of the suspension were applied on a lacey support film. Diffuse reflectance Fourier transform infrared (DRIFT-IR) spectroscopy was performed on a Thermo Scientific Nicolet iS50 FT-IR spectrometer with a MCT detector with a resolution of 2 cm^{-1} and a scanning number of 64. The sample in the form of pellet was degassed under vacuum (10^{-3} Pa) for 1 h at 30 °C in the 10-cm Demountable Gas Cell. Subsequently, the initial background spectrum was recorded. (i) For the time-resolved DRIFT-IR spectra of CO adsorption, a pure CO (99.99%) flow of 10 mL min^{-1} was introduced to the cell for 1 h. Afterwards a He flow of 10 mL min^{-1} was switched to thoroughly purge the free and physisorbed CO molecules. Finally the spectrum was recorded. (ii) For the time-resolved DRIFT-IR spectra of LA conversion, LA was first introduced into the cell by He flow at 30 °C. After the introduction of H$_2$ or He at a pressure of 1 MPa, the cell was heated to 100 °C with a ramp of 20 °C min^{-1}. The spectra of 1300–1900 cm^{-1} with the time on stream were collected. Finally, the cell was cooled to 30 °C and the spectrum was recorded. The background spectra of LA, α-AL and GVL were previously recorded at 30 °C after a He purge for 0.5 h. (iii) For pyridine adsorption FT-IR spectra, the pyridine vapor was introduced to the cell for 0.5 h. Afterwards, a He flow (10 mL min^{-1}) was switched to remove the excessive pyridine for 0.5 h, then the cell was heated to 150 °C (10 °C min^{-1}) and kept for 0.5 h. Finally, the cell was cooled to 30 °C and the spectrum of 1400–1700 cm^{-1} was recorded.

2. Complementary data

Table S1 Catalytic performances of the MIL(Fe), MIL(FeSn$_x$) and MOF(Sn) carriers for hydrogenation of LA

Catalyst	Conv. LA (%)	Select. (%)	
		α-AL	GVL
MIL(Fe)	0	0	0
MIL(FeSn$_{0.1}$)	0	0	0
MIL(FeSn$_{0.2}$)	0	0	0
MIL(FeSn$_{0.3}$)	0	0	0
MOF(Sn)	0	0	0

Reaction conditions: LA, 5 mmol; catalyst, 50 mg; dioxane, 10 mL; H$_2$, 1 MPa; temperature, 100 °C; time, 5 h.

Table S2 Kinetic data for hydrogenation of LA over the Pt@MIL(Fe), Pt@MIL(FeSn$_{0.2}$) and Pt@MOF(Sn) catalysts

T	Conv. LA (%)			k (h^{-1})			1000/T	ln$k$		
(°C)	Pt@MIL(Fe)	Pt@MIL(FeSn$_{0.2}$)	Pt@MOF(Sn)	Pt@MIL(Fe)	Pt@MIL(FeSn$_{0.2}$)	Pt@MOF(Sn)	(K^{-1})	Pt@MIL(Fe)	Pt@MIL(FeSn$_{0.2}$)	Pt@MOF(Sn)
90	13	36[a]	6	0.14	0.45	0.06	2.61	-3.42	-1.45	-4.29
100	22	48[a]	11	0.25	0.65	0.12	2.54	-2.90	-1.00	-3.75
110	29	61[a]	15	0.34	0.94	0.16	2.48	-2.47	-0.64	-3.27

Reaction conditions: catalyst, LA, 5 mmol; 50 mg; dioxane, 10 mL; H$_2$, 1.0 MPa; time, 4 h, [a] 2 h. The rate constant (k) was calculated by lnC_0/lnC_t = kt. The apparent activation energy (E_a) was calculated based on the arrangement of Arrhenius equation, E_a = −Rdln$k$/dln(1/K).

Table S3 Time-course reactions for hydrogenation of LA over the Pt@MIL(FeSn$_{0.1}$) and Pt@MIL(FeSn$_{0.3}$) catalysts

Catalyst	Time (h)	Conv. (%)	Select. (%)	
			α-AL	GVL
Pt@MIL(FeSn$_{0.1}$)	1	16	8	92
	2	31	5	95
	3	45	3	97
	4	57	1	99
	5	68	1	99
Pt@MIL(FeSn$_{0.33}$)	1	19	0	100
	2	36	0	100
	3	51	0	100
	4	64	0	100
	5	76	0	100

Reaction conditions: LA, 5 mmol; catalyst, 50 mg; dioxane, 10 mL; H$_2$, 1 MPa; temperature, 100 ℃.

Table S4 Initial catalytic performances of the Pt@MIL(Fe), Pt@MIL(FeSn$_x$) and Pt@MOF(Sn) catalysts for hydrogenation of LA under harsh reaction conditions

Catalyst	Conv. (%)	Select. (%)	
		α-AL	GVL
Pt@MIL(Fe)	18	0	100
Pt@MIL(FeSn$_{0.1}$)	33	0	100
Pt@MIL(FeSn$_{0.2}$)	56	0	100
Pt@MIL(FeSn$_{0.3}$)	39	0	100
Pt@MOF(Sn)	7	0	100

Reaction conditions: LA, 5 mmol; catalyst, 50 mg; dioxane, 10 mL; H$_2$, 2 MPa; temperature, 120 ℃; time, 1 h.

Table S5 Elemental compositions of the Pt@MIL(Fe), Pt@MIL(FeSn$_x$) and Pt@MOF(Sn) catalysts

Catalyst	Pt (wt.%)[a]	Sn/Fe molar ratio	
		Bulk[a]	Surface[b]
Pt@MIL(Fe)	0.41	–	–
Pt@MIL(FeSn$_{0.1}$)	0.39	0.09	0.07
Pt@MIL(FeSn$_{0.2}$)	0.38	0.16	0.15
Pt@MIL(FeSn$_{0.3}$)	0.40	0.25	0.22
Pt@MOF(Sn)	0.42	–	–

[a] Measured by ICP-MS. [b] Determined by XPS.

Table S6 Textural properties of the MIL(Fe), MOF(Sn) and MIL(FeSn$_{0.2}$) carriers, and the Pt@MIL(FeSn$_{0.2}$) catalyst

Catalyst	S_{BET} (m^2 g^{-1})	$D_{micro-pore}$ (nm)	$D_{meso-pore}$ (nm)
MIL(Fe)	196	–	2.3
MOF(Sn)	49	0.4, 1.2	2.2
MIL(FeSn$_{0.2}$)	458	0.4, 0.5, 0.6, 0.7, 1.0	2.1, 2.7
Pt@MIL(FeSn$_{0.2}$)	400	0.4, 0.5, 0.6, 0.7, 1.0	2.1, 2.8

Table S7 XPS parameters of Pt $4f_{7/2}$, Fe $2p_{3/2}$ and Sn $3d_{5/2}$ lines for the Pt@MIL(Fe), Pt@MIL(FeSn$_x$) and Pt@MOF(Sn) catalysts

Catalyst	Binding energy (eV)					Pt^0/(Pt^0+Pt^{2+}) (%)
	Pt^0	Pt^{2+}	Fe^{2+}	Fe^{3+}	Sn^{4+}	
Pt@MIL(Fe)	71.3	72.5	709.5	711.0	–	65.5
Pt@MIL(FeSn$_{0.1}$)	71.3	72.5	709.6	711.2	486.5	68.3
Pt@MIL(FeSn$_{0.2}$)	71.4	72.6	709.7	711.3	486.4	88.0
Pt@MIL(FeSn$_{0.3}$)	71.4	72.6	709.5	711.1	486.6	82.6
Pt@MOF(Sn)	71.0	72.2	–	–	487.0	71.6

Table S8 Distribution and amount of acidic sites on the Pt@MIL(Fe), Pt@MIL(FeSn$_x$) and Pt@MOF(Sn) catalysts

Catalyst	Acidity (μmol g^{-1})			Lewis acidity/Total acidity (%)
	Lewis	Brønsted	Total	
Pt@MIL(Fe)	254	16	270	94
Pt@MIL(FeSn$_{0.1}$)	277	56	333	83
Pt@MIL(FeSn$_{0.2}$)	530	57	587	90
Pt@MIL(FeSn$_{0.3}$)	258	77	336	77
Pt@MOF(Sn)	238	170	408	58

Table S9 Comparison study on the Pt-supported catalysts for hydrogenation of LA to GVL

Catalyst	Conv. (%)	Select. (%)	Yield (%)	Time (h)	T (°C)	P, H$_2$ (MPa)	TOF (h^{-1})	Reuse times	Reference
Pt@MIL(FeSn$_{0.2}$)	>99	100	>99	5	100	1	1386	5	this work
Pt/Sn$_{0.8}$Mn$_1$O$_y$	99	100	99	6	120	2	2709	10	1
Pt-TiO$_2$/α-Al$_2$O$_3$	98	98	96	1	150	3	4943	5	2
Pt/Al$_2$O$_3$^{a}	94	100	94	5	70	0.13	–	–	3
Pt/zeolite-Y	100	92	92	24	220	2.5	13	–	4
Pt@meso-SiO$_2$	88	98	86	5	150	1	27	3	5

^{a} In the assistance of extra bio-reductants.

References:

1. Y. Lu, Y. Wang, Q. Tang, Q. Cao and W. Fang, Appl. Catal. B, 2022, 300, 120746.
2. F. Meng, X. Yang, S. Zhao, Z. Li, G. Zhang, Y. Qi, S. Chu, G. Wang, J. Zhang, Y. Qin and B. Zhang, Appl. Catal. B, 2023, 324, 122236.
3. R. Y. Parapat, F. A. Yudatama, M. R. Musadi, M. Schwarze and R. Schomäcker, Ind. Eng. Chem. Res., 2019, 58, 2460.
4. H.-T. Vu, F. M. Harth and N. Wilde, Front. Chem., 2018, 6, 143.
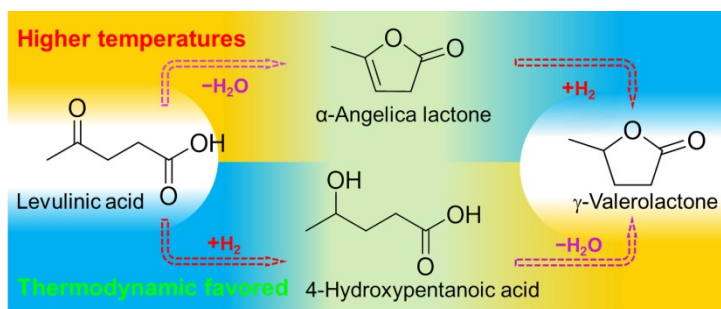5. M. Nemanashi, J.-H. Noh and R. Meijboom, Appl. Catal. A, 2018, 550, 77.

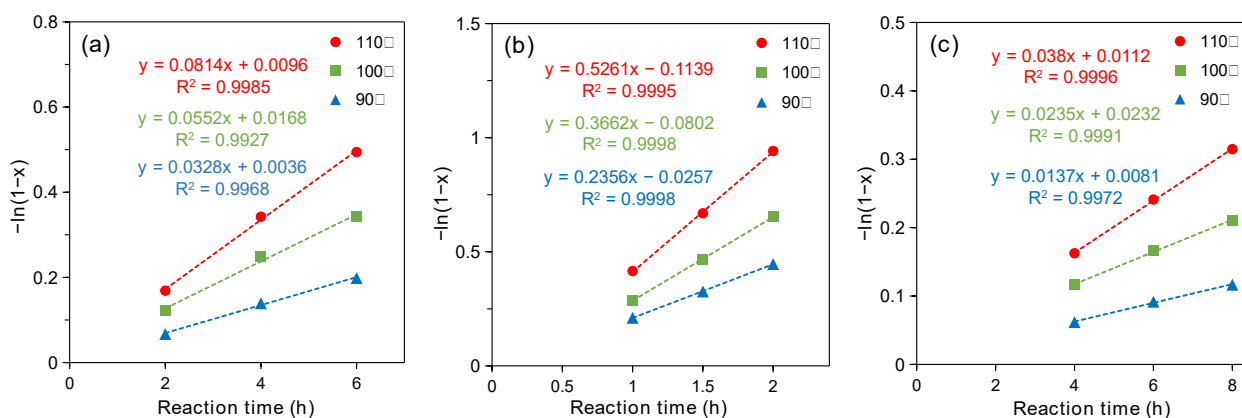**Fig. S1** Reaction pathway for chemical conversion of levulinic acid into γ-valerolactone.

Fig. S2 Kinetic profiles for hydrogenation of LA over the (a) Pt@MIL(Fe), (b) Pt@MIL(FeSn$_{0.2}$), and (c) Pt@MOF(Sn) catalysts. Reaction conditions: LA, 5 mmol; catalyst, 50 mg; dioxane, 10 mL; H$_2$, 1 MPa.
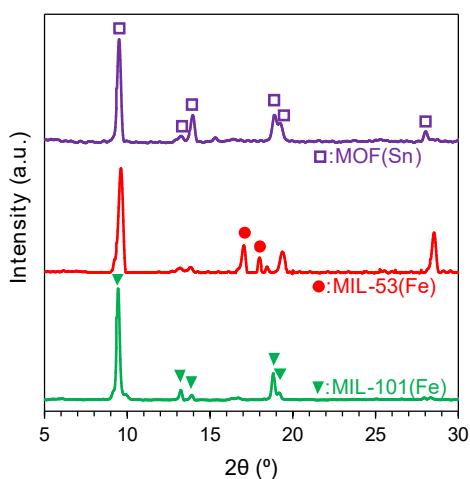

Fig. S3 XRD patterns of the (a) Pt@MIL(Fe), (b) Pt@MIL(FeSn$_{0.2}$), and (c) Pt@MOF(Sn) catalysts.
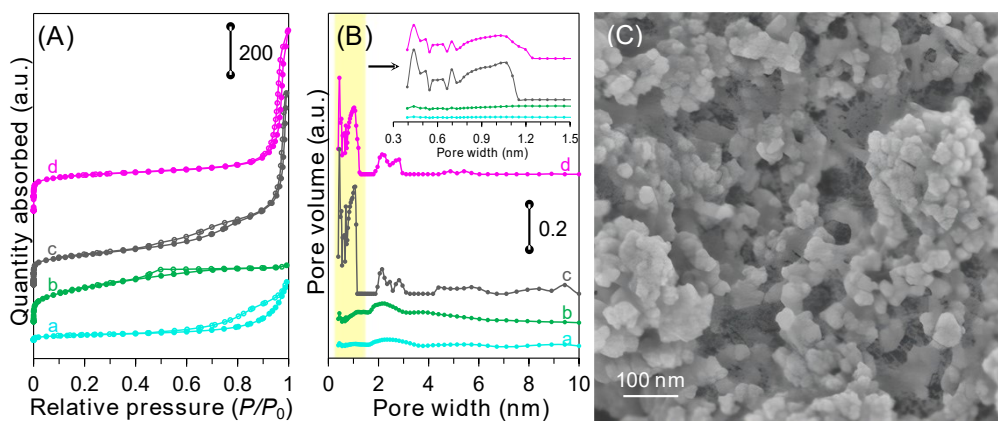
Fig. S4 (A) N_2 adsorption-desorption isotherms and (B) the corresponding pore size distributions of (a) MIL(Fe), (b) MOF(Sn), (c) MIL(FeSn$_{0.2}$), and (d) Pt@MIL(FeSn$_{0.2}$). (C) SEM image of MIL(FeSn$_{0.2}$).
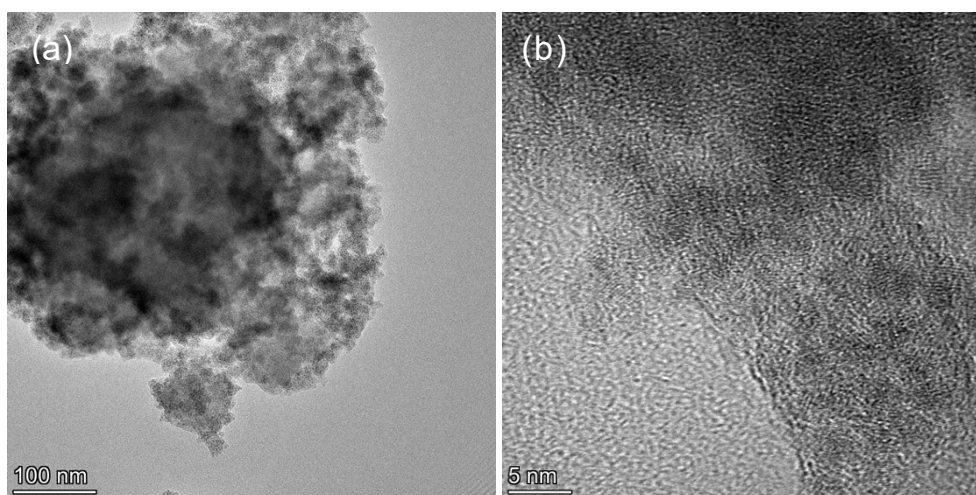

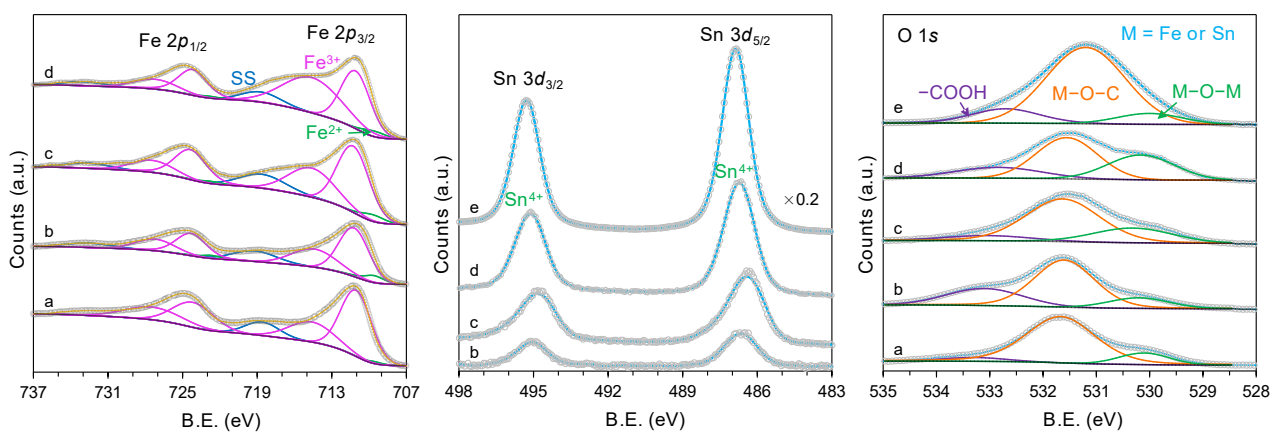**Fig. S5** (a) TEM and (b) HR-TEM images of the Pt@MIL(FeSn$_{0.2}$) catalyst.

Fig. S6 Deconvoluted XPS spectra of the Fe 2p, Sn 3d and O 1s core levels for the (a) Pt@MIL(Fe), (b) Pt@MIL(FeSn$_{0.1}$), (c) Pt@MIL(FeSn$_{0.2}$), (d) Pt@MIL(FeSn$_{0.3}$), and (e) Pt@MOF(Sn) catalysts.

The used Pt@MIL(FeSn$_{0.2}$) catalyst after certain post-treatment (see experimental details) is tested in consecutive recycling experiments and shows remarkable stability after five cycles under the regular reaction conditions (Fig. S7a). Furthermore, the stability is also verified within the kinetic-controlled region, because any deactivation of a catalyst can be easily reflected during the initial stage. Then the possible leaching of Pt from the catalyst is investigated by a hot-filtration process. Conversion of LA and distribution of products are found to be unchanged when the catalyst is removed at 1 h and the remaining liquid is stirred at 100 °C in the presence of H$_2$ for another 5 h (Fig. S7b). This result indicates no loss of active Pt component from the catalyst into the reaction mixture. It is no significant change in the position and valence state of Pt after the reaction. This may be responsible for the superior stability and reusability of the Pt@MIL(FeSn$_{0.2}$) catalyst.
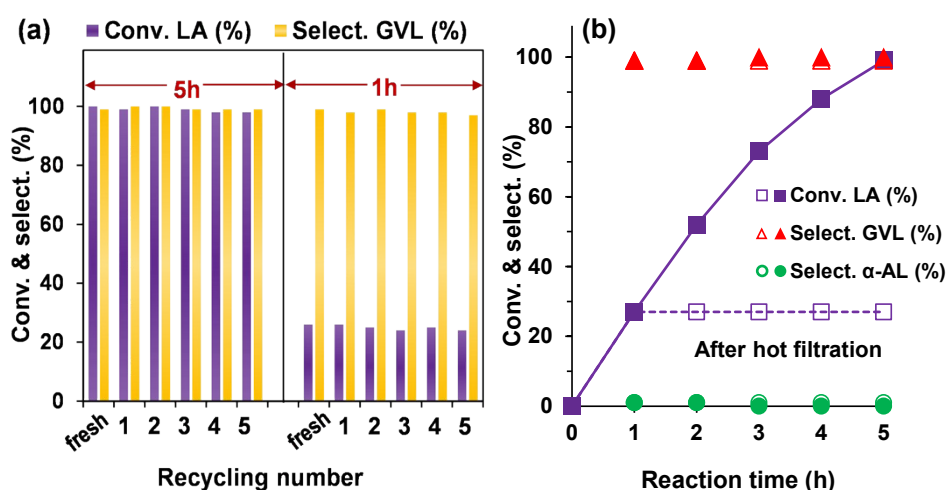

Fig. S7 (a) Consecutive recycling test under the optimized reaction conditions (5 h) and within the kinetic-controlled region (1 h), and (b) leaching test after hot filtration for the Pt@MIL(FeSn$_{0.2}$) catalyst for hydrogenation of LA. Reaction conditions: LA, 5 mmol; catalyst, 50 mg; dioxane, 10 mL; H$_2$, 1 MPa; temperature, 100 °C.